Available online at www.sciencedirect.com

jmr&t
Journal of Materials Research and Technology
www.jmrt.com.br

Original Article

Cold-rolled multiphase boron steels: microstructure and mechanical properties

Fábio Dian Murari[a], *André Luiz Vasconcelos da Costa e Silva*[b], *Roberto Ribeiro de Avillez*[c,*]

[a] *Usiminas Technology Center, Ipatinga, MG, Brazil*
[b] *Escola de Engenharia Industrial Metalúrgica, Universidade Ferderal Fluminense (UFF), Volta Redonda, RJ, Brazil*
[c] *Pontifícia Universidade Católica do Rio de Janeiro (PUC-Rio), Rio de Janeiro, RJ, Brazil*

ARTICLE INFO

Article history:
Received 15 October 2014
Accepted 3 December 2014
Available online 15 January 2015

Keywords:
Multiphase steels
Boron
Thermo-Calc®
Dilatometry

ABSTRACT

The influence of the boron concentration on phase transformation characteristics, microstructure and mechanical properties of multiphase steels was investigated using computational thermodynamics (Thermo-Calc®), dilatometry, quantitative metallography and tensile tests. Pilot scale 50 kg steel ingots were prepared in an induction furnace operating under an argon gas atmosphere with boron contents between 0 and 47 ppm. The ingots were cut into 35 mm thick blocks, which were reheated to 1250 °C for 1 h and hot rolled for seven passes to attain a thickness of 7.0 mm. The hot-rolled sheets were machined and then cold rolled to a final thickness of 1.2 mm. Continuous annealing cycles were performed in a Bähr dilatomer and in a Gleeble machine. Continuous annealing laboratory simulations showed that boron did not significantly influence the amount of austenite formed during heating and soaking steps. However, boron influenced austenite transformation during the cooling step, which reduced the amount of ferrite and increased the amount of bainite. Regarding the mechanical properties, adding boron increased strength and decreased ductility of the product. The steels with boron concentrations up to 27 ppm exhibited the greatest effect. The amount of austenite, which was calculated using Thermo-Calc®, was slightly overestimated compared with that obtained by dilatometry and metallography, particularly for soaking temperatures lower than 800 °C.

1. Introduction

Advanced high-strength steels with multiphase microstructures, which consist of ferrite, bainite, martensite and retained austenite, are being used increasingly more in many automotive applications; in particular, these steels are replacing conventional HSLA steels due to their more desirable strength–ductility ratio. These materials are characterized by an interesting combination of high strength, good ductility,

* *Corresponding author.*
E-mail: avillez@puc-rio.br (R.R. de Avillez).
http://dx.doi.org/10.1016/j.jmrt.2014.12.001

Table 1 – Chemical composition of the multiphase steels used in the study (in weight percent).

Steel	C	Mn	Si	P	S	Al	B	Nb + Ti	N	Ti/N
B10	0.10	1.8	0.5	0.02	0.007	0.029	0.0013	>0.028	0.0052	4.4
B30	0.11	1.8	0.5	0.02	0.005	0.025	0.0027		0.0042	4.5
B50	0.09	1.8	0.5	0.02	0.007	0.034	0.0047		0.0051	4.7
Base	0.09	1.8	0.3	0.01	0.005	0.043	–	–	0.0043	–

continuous yielding, high initial work hardening rates (n values) and a low yield stress to tensile strength ratio (YS/TS) [1].

In the context of multiphase steels, boron is an unique alloying element in that a soluble content of 0.0010–0.0030% can provide a hardenability effect equivalent to adding approximately 0.5% of other elements, such as manganese, chromium or molybdenum [2–6]. Thus, various approaches have been attempted to produce multiphase steels with boron additions with the objective of reducing costs.

It is generally accepted that at the fully austenitized condition, boron segregation or the precipitation of fine $Fe_{23}(C, B)_6$ carbides during cooling at austenite grain boundaries retards the transformation from austenite to ferrite by impeding the nucleation of ferrite, which subsequently improves the hardenability of steel [7,8]. In the production of multiphase steels, inhibiting ferrite formation is expected to increase the amount of martensite or bainite. However, for multiphase steels, ferrite grows during cooling from the $(\alpha + \gamma)$ phase

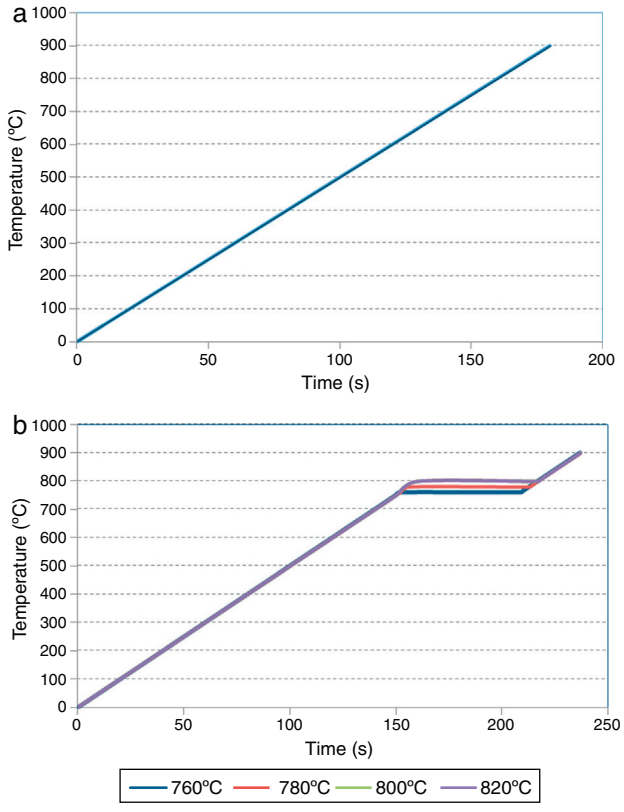

Fig. 1 – (a) Thermal cycles conducted in the Bähr dilatometer to determine the volume fraction of austenite formed with heating steps; (b) heating with the soaking steps.

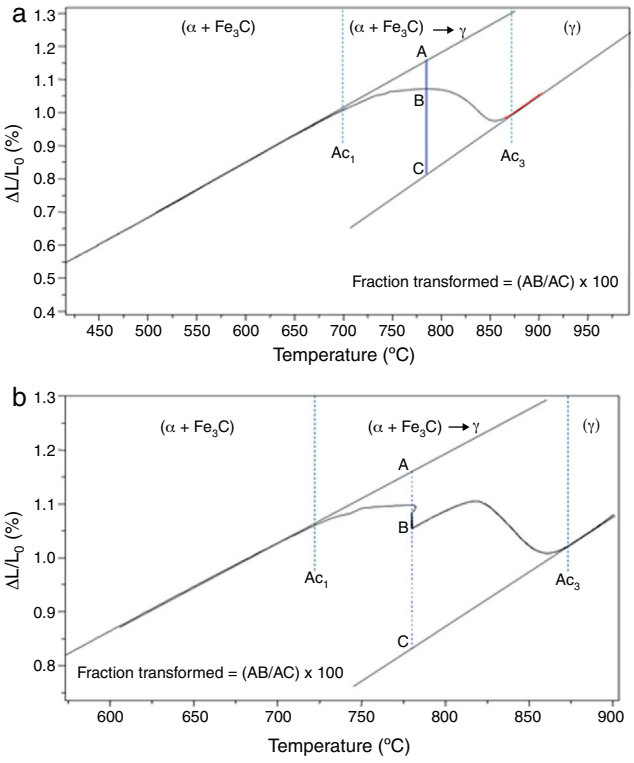

Fig. 2 – Example of application of the lever rule to determine the fraction of transformed austenite by means of dilatometry. (a) Continuous heating; (b) heating with the soaking step.

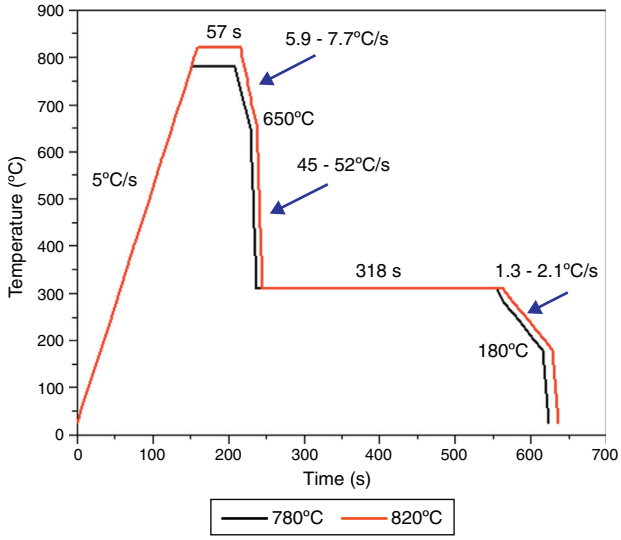

Fig. 3 – Continuous annealing cycles performed in the Gleeble simulator.

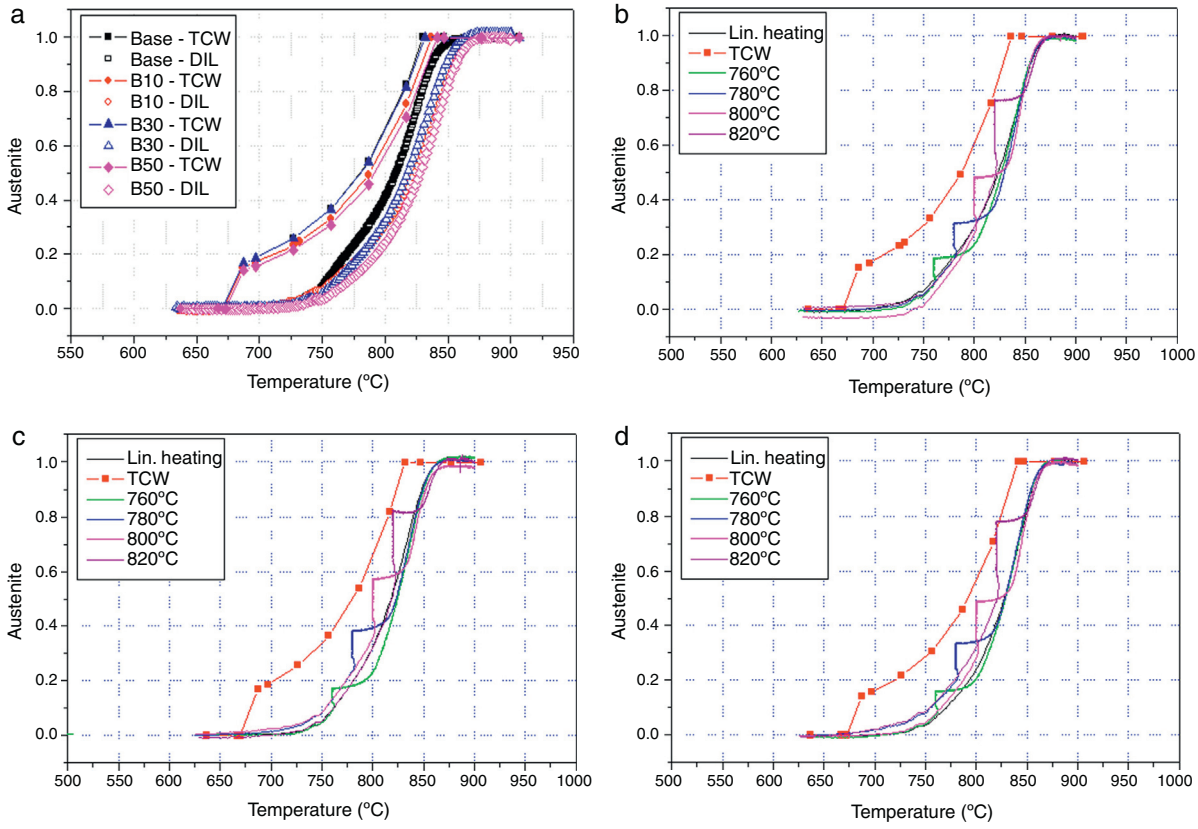

Fig. 4 – Volume fraction of austenite formed during heating and soaking steps determined by Thermo-Calc® (TCW) and dilatometry (DIL) for different boron additions. (a) Base metal; (b) 10 ppm boron; (c) 30 ppm boron; (d) 50 ppm boron.

field from the already existing ferrite. Nucleation of new ferrite grains, which has been observed in several instances, does not contribute significantly to the kinetics of ferrite formation while cooling the ($\alpha + \gamma$) mixture. Nevertheless, because the energy of the α/γ interface is comparable to that of the γ/γ grain boundary, it could be expected that boron redistributes from prior austenite grain boundaries to α/γ interfaces during intercritical annealing. If this occurs, the boron would then interfere with the growth mechanisms of ferrite into austenite during subsequent cooling [9].

In the present work, the influence of boron content on the phase transformation behavior, microstructure and mechanical properties of multiphase steels, which were intercritically annealed, was investigated by dilatometry, quantitative metallography, tensile tests and computational thermodynamics.

2. Experimental setup

For this study, four 50 kg ingots were prepared in a vacuum induction furnace with the chemical composition shown in Table 1. The ingots were cut into blocks that were 35 mm thick and were reheated to 1250 °C for 1 h and hot rolled in seven passes to obtain a 7.0 mm thickness. The hot-rolled sheets were machined to obtain flat, clean surfaces and then cold rolled to a final thickness of 1.2 mm.

The formation of austenite during the heating step in the continuous annealing process was studied by means of equilibrium computational thermodynamics (Thermo-Calc® 5.0 [10] and the thermodynamic database, TCFE6[1]). These values were compared with the dilatometry results and the quantitative metallography results of the samples, where optical and scanning electron microscopy were used for the characterization. For the dilatometry, the lever rule was used, and cycles both with and without the soaking step (Figs. 1 and 2) were considered. The cooling rates obtained by water quenching were always greater than 500 °C/s to ensure that the austenite present at the high temperature would transform into only martensite or bainite and that no pearlite would be present, which meant that the volume fraction of austenite formed during heating/soaking could be indirectly determined. For this purpose, the specimens were etched with LePera's agent, which left martensite and retained austenite (MA) white, whereas the other constituents were painted in different colors. The volume fractions of the constituents were measured by image analyzer software.The samples for the tensile tests had a gauge length of 25 mm that was transversal to the rolling

[1] Thermo-Calc Software Database TCFE6 Steels/Fe-alloys database version 6.

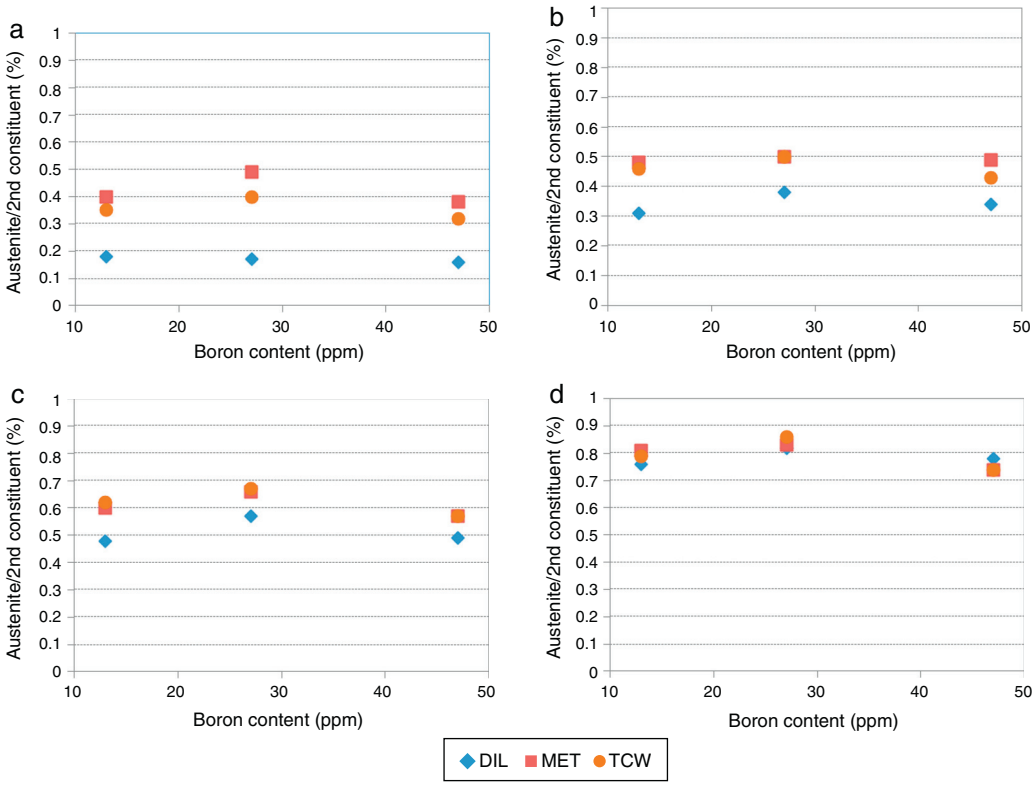

Fig. 5 – Results of the quantitative analysis of the constituents. Comparison between the different measurement methods and the results obtained by Thermo-Calc® at two different soaking temperatures. (a) 760 °C; (b) 780 °C; (c) 800 °C; (d) 820 °C.

direction and were machined from the cold-rolled samples to evaluate the mechanical properties.To better simulate the actual cycles encountered in the industrial line of continuous annealing, Gleeble tests were also performed. As shown in Fig. 3, the cycles were chosen based on typical industrial line parameters. Metallographic samples of the tensile tests were prepared following standard metallographic procedures and examined by optical and scanning electron microscopes. To determine the volume fraction of polygonal ferrite (PF) and the second constituent, a 4% Nital etchant was used, and LePera etchant was applied to highlight the MA constituent. The volume fractions of bainite and the undissolved carbides (B + C) were determined by the difference between the volume fractions of the second constituent and that of MA.

3. Experimental results

Fig. 4a shows the austenite fractions formed during heating, which were obtained from two different methods: using Thermo-Calc® (TCW) and experimentally determined by dilatometry (DIL). The dilatometric experiments that included the soaking step are shown in Fig. 4b–d and compared with the equilibrium calculations. As seen from Fig. 4a, the amount of austenite calculated with the Thermo-Calc® for a given intercritical temperature is greater than the experimental value determined by dilatometry. This result was expected because the Thermo-Calc calculations considered the condition of thermodynamic equilibrium. Therefore, it is likely that a kinetic effect during heating slows the growth of austenite, and equilibrium did not occur. Regarding the effect of boron, the addition of this element did not significantly influence the amount of austenite formed during heating. The small variations that did occur are most likely due to differences in the levels of other elements, such as carbon, aluminum and nitrogen. Furthermore, the amount of austenite determined by dilatometry at 820 °C was equal to the equilibrium value calculated with Thermo-Calc®. This result shows that the kinetics of austenite growth occurs rapidly and thus, is able to reach equilibrium for typical industrial heating cycles. Therefore, it is possible to infer that the state of thermodynamic equilibrium was reached for temperatures at approximately 850 °C for the present alloys during the uniform heating cycle. Fig. 4b–d shows the effect of the soaking treatment, which causes the amount of austenite to approach its equilibrium values for 57 s of soaking at 820 °C. Fig. 5 shows the amount of austenite after being water quenched from the soaking temperature determined from both dilatometry and quantitative metallography (MET). The values obtained by quantitative metallography were always greater than those obtained by dilatometry. However, the quantitative metallography results also had larger errors due to surface sampling compared with those of the volumetric dilatometry measurement. As the soaking temperature increased, the difference between the results of the two experimental methods decreased. Fig. 5a–d

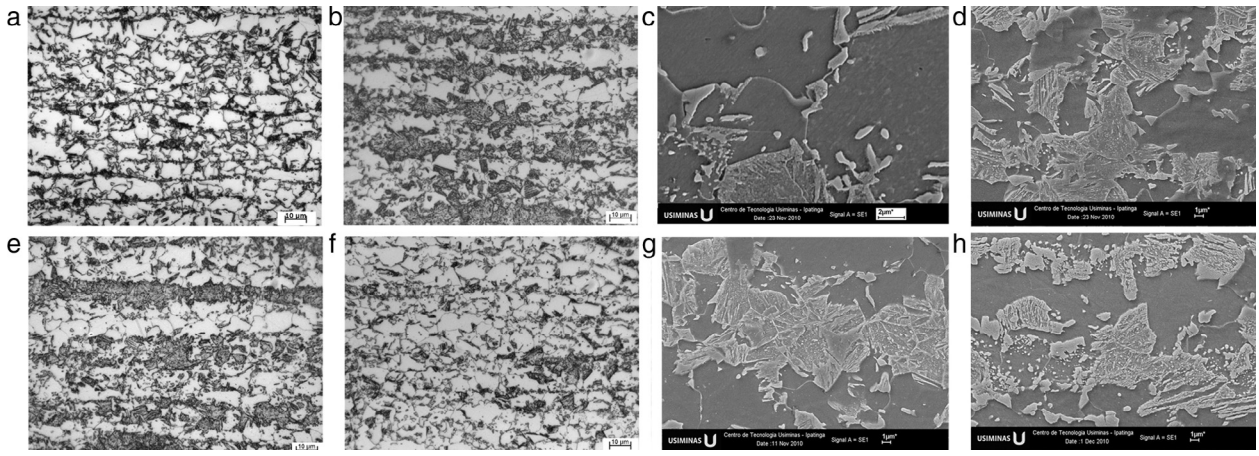

Fig. 6 – Microstructural aspect of the studied steels. Soaking temperature: 820 °C. Overaging temperature: 300 °C. Metallographic etching: Nital. Analysis performed at 1/4 thickness. (a) Base metal, optical microscopy; (b) 10 ppm boron, optical microscopy; (c) base metal, scanning electron microscopy; (d), 10 ppm boron, scanning electron microscopy; (e) 30 ppm boron, optical microscopy; (f), 50 ppm boron, optical microscopy; (g) 30 ppm boron, scanning electron microscopy; (h), 50 ppm boron, scanning electron microscopy.

does not reveal any effect that can be ascribed to the boron addition on the austenite growth while being heated or soaked.

Fig. 6 shows the microstructure of the four steels after simulation of the cycles shown in Fig. 3. The more magnified micrographs (scanning electron microscopy) in this figure suggest that the amount of constituents does not seem to depend on the boron amount. However, the quantitative metallography results presented in Fig. 7 show that the increase in boron (up to approximately 30 ppm) initially decreased the amounts of the ferrite and MA constituents, which resulted in an increase in the amount of the second constituents, in particular, bainite. Hence, boron has a strong effect during cooling.

The mechanical properties for the as-annealed material shown in Fig. 8 follow the expected behavior due to the microstructure. The increase in boron content up to 27 ppm caused an increase in the yield stress and tensile stress and decreased the total elongation, which is due to the increase in the amount of the second constituent.

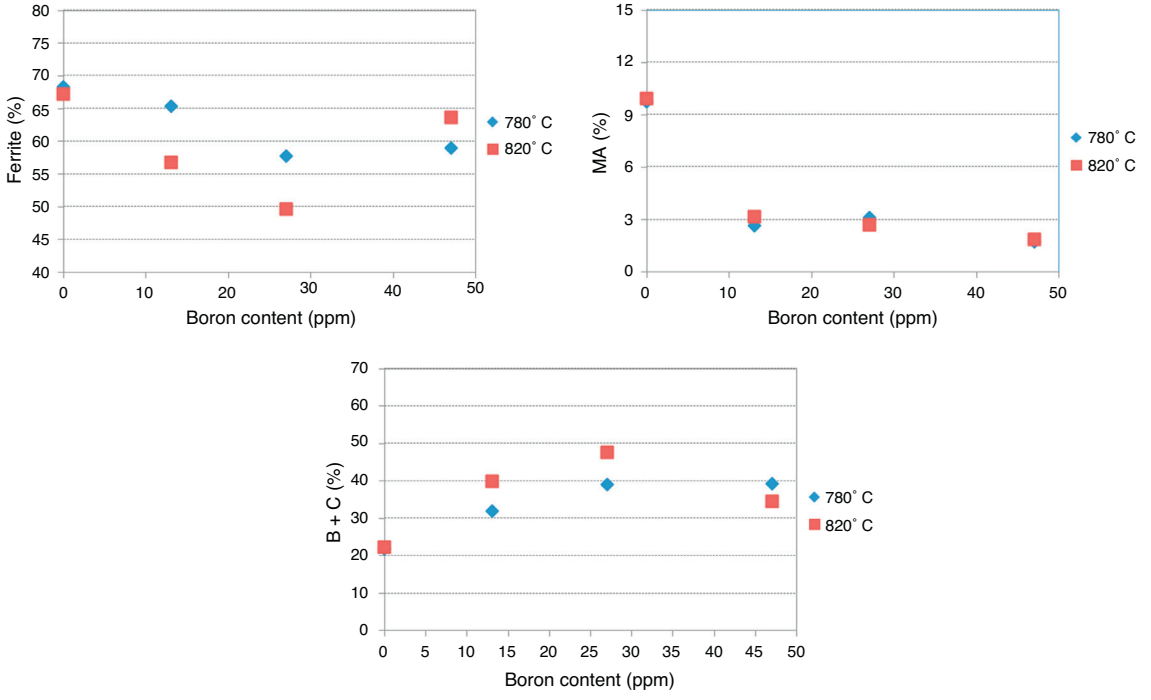

Fig. 7 – Changes in the amounts of the constituents with the addition of boron at different soaking temperatures.

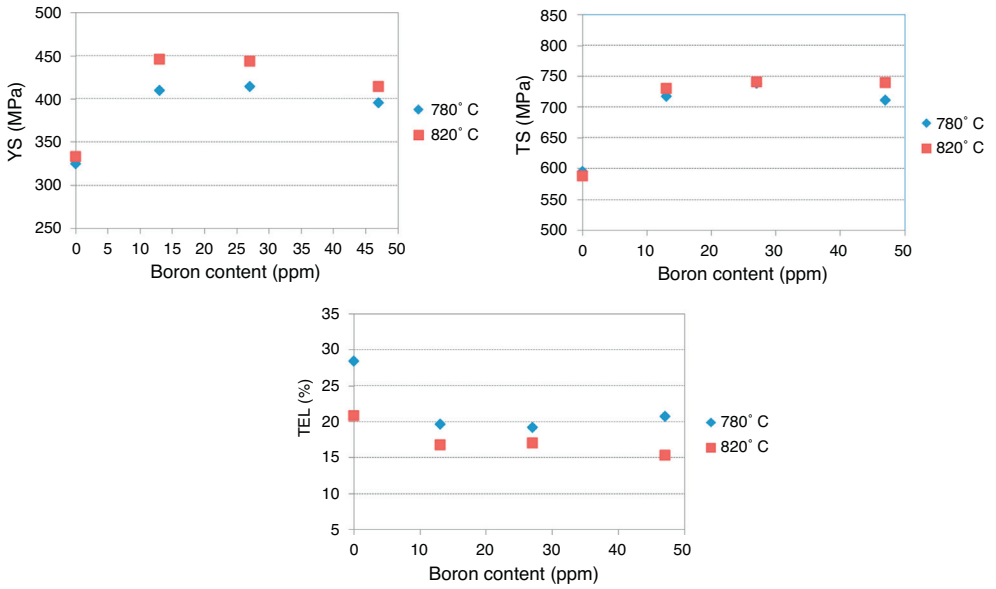

Fig. 8 – Changes in mechanical properties with different boron concentrations at different soaking temperatures.

4. Conclusions

The effects of the austenitizing temperature on the final microstructure of industrial steels modified by adding boron were evaluated by dilatometry and quantitative microscopy and compared with thermodynamic equilibrium calculations. Boron had no measurable effect on the behavior during the austenitization cycle. Equilibrium conditions were obtained after soaking for 57 s at 820 °C. Therefore, equilibrium thermodynamics may be used to determine the austenitization temperature and could be used during the development stage of alloy design.

At lower temperatures and shorter austenization times, the equilibrium calculations overestimated the amount of austentite compared with the values obtained by dilatometry. Therefore, an appropriate model to predict the volume fraction of austenite during heating should consider the diffusional growth of austenite.

In the final microstructure, the addition of boron up to 27 ppm reduced the amount of ferrite, which increased the amount of bainite. The martensite amount decreased as the boron content increased. The increase in the soaking temperature, from 780 °C to 820 °C, also increased the amount of bainite.

The mechanical properties reflected the increase in the bainite fraction, which were determined by microstructural characterization; the mechanical resistance increased and the ductility decreased up to 27 ppm of boron.

Conflicts of interest

The authors declare no conflicts of interest.

Acknowledgement

Roberto Ribeiro de Avillez thanks CNPq for partial funding.

REFERENCES

[1] Samek L, De Moor E, Penning J, Speer JG, Cooman BC. Static strain aging of microstructural constituents in transformations-induced-plasticity steel. Metall Mater Trans A 2008;A39:2542–54.
[2] Llewellyn DT, Hillis DJ. Dual phase steels. Ironmak Steelmak 1996;23:471–8.
[3] Bhadeshia HKDH, Svensson LE. Model for boron effects in steel welds. In: International conference on modeling and control of joining processes. 1993. p. 153–60.
[4] Melloy GF. In: Leslie WC, editor. The physical metallurgy of steels. International student edition New York: McGraw-Hill International Book Company; 1981. p. 269–81.
[5] Kapadia BM, Brown RM, Murphy WJ. Trans the influence of nitrogen, titanium and zirconium on the boron hardenability effect in constructional steels. TMS-AIME 1969:242.
[6] Llewellyn DT, Cook WT. Metallurgy of boron treated low alloy steels. Met Technol 1974;1:517–29.
[7] Akselsen OM, Grong O, Kvaale PE. A comparative study of the heat affected zone (HAZ) properties of boron containing low carbon steel. Metall Trans A 1986;A17:1529–36.
[8] Pressouyre GM, Primon G, Blondeau R. Recent developments in HSLA boron steels. In: HSLA steels: metallurgy and applications. Proceedings of Metals Park: ASM International; 1986. p. 335–50.
[9] Shen XP, Priestner R. Effect of boron on the microstructure and tensile properties of dual phase steel. Metall Trans A 1990;A21:2547–53.
[10] Andersson JO, Helander T, Höglund L, Shi PF, Sundman B. Thermo-Calc and DICTRA, computational tools for materials science. Calphad 2002;26:273–312.